Journal of Alloys and Compounds 679 (2016) 26–31

Contents lists available at ScienceDirect

Journal of Alloys and Compounds

journal homepage: http://www.elsevier.com/locate/jalcom

Effects of B_2O_3 addition on sintering behavior and microwave dielectric properties of ixiolite-structure $ZnTiNb_2O_8$ ceramics

Haitao Wu*, Quanjing Mei, Chunfang Xing, Jinxin Bi

School of Materials Science and Engineering, University of Jinan, Jinan 250022, China

ARTICLE INFO

Article history:
Received 20 September 2015
Received in revised form
6 March 2016
Accepted 5 April 2016
Available online 7 April 2016

Keywords:
$ZnTiNb_2O_8$
Microstructures
Microwave dielectric properties
B_2O_3 addition

ABSTRACT

The effects of B_2O_3 additives on the sintering behavior, microstructure and microwave dielectric properties of ixiolite-structure $ZnTiNb_2O_8$ ceramics prepared by conventional solid-state route were investigated. The B_2O_3 additives, acting as a sintering aid, can effectively decrease the sintering temperature of $ZnTiNb_2O_8$ ceramics to 1050 °C, due to the formation of liquid phase. Little second phase from XRD results was observed throughout the entire experiments. The variations in the dielectric constant (ε_r) and quality factor ($Q\cdot f$) of the ixiolite-structure $ZnTiNb_2O_8$ ceramics were studied systematically depending on the adopting of B_2O_3 and the sintering temperatures. With the increase of the B_2O_3 addition, ε_r and $Q\cdot f$ decreased and the temperature coefficient of resonant frequency (τ_f) slightly fluctuated around −20 ppm/°C. The optimal microwave dielectric properties with high ε_r ~35.04, $Q\cdot f$ ~50,100 GHz, and a near-zero τ_f ~−20.21 ppm/°C were obtained at 1 wt%-B_2O_3-doped samples sintered at 1050 °C. The relatively low sintering temperature and high dielectric properties in microwave range would make $ZnTiNb_2O_8$ ceramics promising for application in electronics.

1. Introduction

In recent years, microwave dielectric materials play an important role in wireless industry with a wide range of applications from microwave tele-communication to intelligent transport systems. They were widely applied in mobile and satellite communications such as filters, dielectric resonators and antennas [1–3]. Generally, the electronic components should possess excellent microwave dielectric properties, such as a high relative permittivity ($\varepsilon_r > 20$), a low dielectric loss ($Q > 5000$, where $Q = 1/\tan\delta$) and a near-zero temperature coefficient of resonant frequency (τ_f) [4].

Among several kinds of dielectric ceramics ixiolite-structure $ZnTiNb_2O_8$(ZTN) ceramics became a kind of well-known dielectric ceramics promisingly, due to high quality factors and an appropriate dielectric constant. And more recently, much attention has been paid on its microwave dielectric properties. For instance, Liao et al. [5] reported that the orthorhombic ixiolite structure ZTN belongs to the space group *Pbcn* (D_{2h}^{14}) and contains one $ZnTiNb_2O_8$ molecule per primitive cell ($3 \times 3 \times 3$). In our previous work [6] the crystal cell parameters of $ZnTiNb_2O_8$ ceramics were a = 4.674 Å, b = 5.659 Å, c = 5.017 Å, with the same α, β, γ angle of 90° and the direct cell volume was 132.7208 $Å^3$. Though $ZnTiNb_2O_8$ ceramics has a ε_r of 34, a $Q\cdot f$ of 42,500 GHz and a τ_f of −52 ppm/°C, the sintering temperature (about 1250 °C) was too high to be applied in wireless communication systems by the solid-state method. Obviously, high sintering temperatures would limit their applications and the reduction of sintering temperature was imperative to the further commercial applications.

Generally, in order to reduce sintering temperatures and improve sintering ability of the $ZnTiNb_2O_8$, there are several approaches: (i) the usage of smaller particle size of starting materials synthesized by chemical processes and (ii) the addition of low-melting glasses, oxides or mixed-oxides. Chemical processing or special methods are often time consuming and expensive. In contrast, the addition of low-melting glasses or mixed-oxides is known to be the most popular method for achieving densified ceramics. Therefore, much attention has been paid to using various sintering aids such as Zn–B–Si(ZBS), Li_2CO_3–H_3BO_3, MgO–CaO–Al_2O_3–SiO_2, and CaO–B_2O_3–SiO_2 in the dielectric ceramics [7–10] and among all sintering fluxes B_2O_3 is commonly recognized as a good additive. However, few researches about the B_2O_3 addition on microwave dielectric properties and microstructure were reported in the present literature for $ZnTiNb_2O_8$ ceramics. In this work, the B_2O_3-doped ZTN ceramics were synthesized through the

* Corresponding author.
E-mail address: msse_wuht@ujn.edu.cn (H. Wu).

http://dx.doi.org/10.1016/j.jallcom.2016.04.046
0925-8388/

solid method. The X-ray diffraction, scanning electron microscope and energy dispersive X-ray spectroscopy were carried out to investigate the correlations between the crystalline structure and microwave dielectric properties of $ZnTiNb_2O_8$ ceramics.

2. Experimental

The $ZnTiNb_2O_8$ ceramics were prepared by a conventional solid-state method. High-purity oxides including ZnO (99.9%), TiO_2 (99.99%) Nb_2O_5 (99.9%) and H_3BO_3 were used as raw materials to prepare the ZTN ceramics. Firstly, stoichiometric amounts of the chemical powders were weighed and ball-milled in a teflon jar with zirconia balls for 8 h. Then all the slurries were dried in an oven in the temperature of 80 °C. Secondly, the mixed powders were pre-sintered at 1000 °C for 2 h and then re-milled for 4 h. Thirdly, the powders were mixed with paraffin wax as a binder granulated and pressed into cylindrical disks of 10 mm diameter and about 5 mm height at a pressure of 6 MPa. These pellets were then preheated at 500 °C for 4 h to expel the binder. Finally, these pellets were sintered at different temperatures of 1000 °C, 1050 °C, 1100 °C, and 1150 °C for 4 h at a heating rate of 5 °C/min.

The apparent densities of the sintered specimens were measured by Archimedes' method. The crystalline structure analysis of the ZTN ceramic was identified by a X-Ray diffractometer (Model D/MAX-B, Rifaku Co., Japan) using Ni filtered Cu Kα radiation ($\lambda = 0.1542$ nm, 40 kV, 20 mA, $2\theta = 15°–75°$). Its morphology and grain size were examined by field emission scanning electron microscopy (Model JEOL JSM-7600F, FEI Co.,Japan). A network analyzer (N5234A, Agilent Co., America) was used for the measurement of microwave dielectric properties. The dielectric constant was measured using Hakki-Coleman post-resonator method by exciting the TE011 resonant mode of a dielectric resonator by using an electric probe as suggested by Hakki and Coleman [11]. Unloaded quality factors were measured using the TE01d mode by the cavity method [12]. All measurements were carried out at room temperature and at frequency of 8–12 GHz. Temperature coefficients of resonant frequency were measured in the temperature range of 25–85 °C. The resonant frequency was noted at regular intervals in the course of heating and the τ_f was calculated using the following Eq. (1):

$$\tau_f = \frac{f_2 - f_1}{f_1(T_2 - T_1)} \quad (1)$$

Where f_1 is the resonant frequency at temperature T_1 and f_2 at temperature T_2.

3. Results and discussion

The apparent densities and diametric shrinkage ratio of ceramics sintered for 4 h with different B_2O_3 contents as a function of sintering temperatures are shown in Fig. 1, through which the optimal sintering temperature could be determined. As shown in Fig. 1(a), the apparent density of ZTN ceramics with different amount of B_2O_3 addition all increased steadily with the increase of sintering temperature firstly, then decreased slightly, and the maximum values were obtained at 1050 °C. For the ceramics with 1 wt% B_2O_3 addition, the densities increased from ~4.63 to ~4.99 g/cm^3 with temperature increasing in the region of 1000–1050 °C, which was about 93.51% of the theoretical density (5.336 g/cm^3) [6]. Based on the result of sintering characteristics, it was concluded that small amount of B_2O_3 addition was able to reduce the sintering temperature due to the melting of B_2O_3 at 445 °C, which would form liquid phase during the sintering process. The liquid spreads to cover the solid surfaces, works as the liquid bridge between

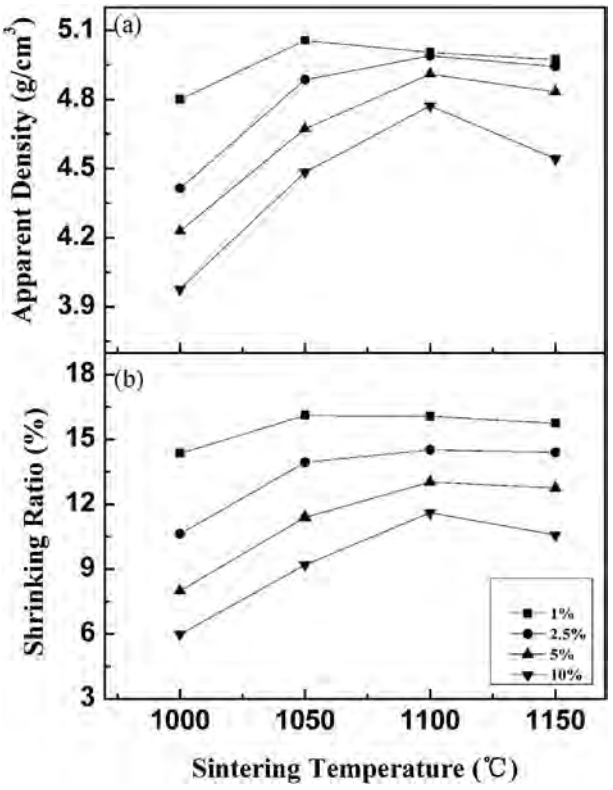

Fig. 1. The apparent densities and diametric shrinkage ratio of $ZnTiNb_2O_8$ ceramics with different B_2O_3 contents as a function of sintering temperature.

particles during liquid phase sintering. However, the apparent density decreased when the amount of B_2O_3 additions over 1 wt%. The grains grew so fast due to the excess liquid phase that cannot adjust to reach the dense arrangement. The pores were closed rapidly and even wrapped inside the grains, so that density of ceramics decreased gradually along with the increase of the amount of B_2O_3 doping.

The shrinkage ratio was characterized by the variation of diametric size before and after the ceramic sintering and showed a similar tendency with apparent densities, as can be seen in Fig. 1(b). Based on the result of shrinkage ratio of ZTN ceramics, it was concluded that a nearly full densification could be obtained for the samples with 1 wt% B_2O_3 addition and the optimal sintering temperature was determined to be 1050 °C for the $ZnTiNb_2O_8$ compounds.

Fig. 2 shows the X-ray diffraction patterns of $ZnTiNb_2O_8$ ceramics with 1 wt% B_2O_3 addition at different sintering temperatures for 4 h. It was found that the crystallization of ixiolite-structure ZTN was in agreement with the XRD pattern of JCPDS No. 48-0323. The predominant phases were identified as the ixiolite-structure $ZnTiNb_2O_8$ with the space group of *Pbcn*(60) and only little secondary phase of the orthorhombic-structure $Zn_{0.17}Ti_{0.33}Nb_{0.5}O_2$ (*P*42/*mnm*(136)) existed at 1000 °C. The X-ray diffraction patterns of $ZnTiNb_2O_8$ ceramics did not have significant change throughout the sintering temperature ranging from 1050 to 1150 °C. Meanwhile, the XRD patterns of ZTN became sharper in view of diffraction peaks from significant lattice planes, such as (111), (110), (023). Moreover, the second phase $Zn_{0.17}Ti_{0.33}Nb_{0.5}O_2$ disappeared with the increase of sintering temperature. Therefore, according to XRD result it was indicated that sintering temperature of synthesizing ixiolite-structure ZTN phase was remarkably decreased to 1050 °C, which was lower than the conventional mixed oxide route

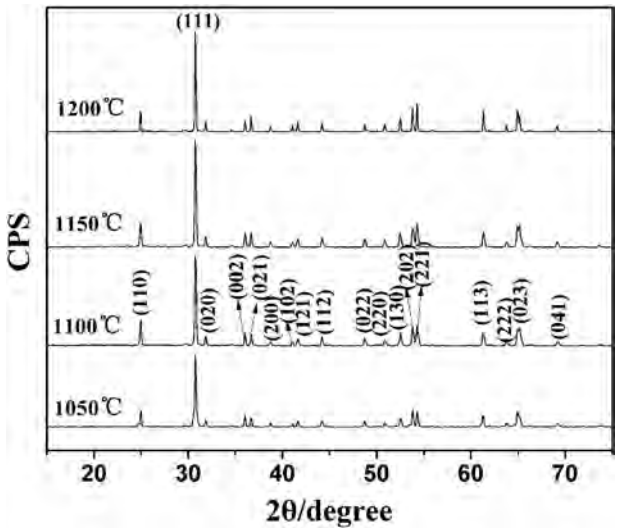

Fig. 2. The X-ray diffraction patterns of $ZnTiNb_2O_8$ ceramics with 1 wt% B_2O_3 addition at different sintering temperatures.

reported earlier [13–17].

The X-ray diffraction patterns of the $ZnTiNb_2O_8$ samples with different amounts of B_2O_3 additive sintered at 1050 °C are shown in Fig. 3. It was observed that all the compounds exhibited a single ZTN phase, from 1% to 10% addition of B_2O_3, and just little secondary phase could be detected. In addition, with the increase of B_2O_3 doping amount, the diffraction peak intensity was slightly enhanced, suggesting that B_2O_3 can promote grain growth. Meanwhile B_2O_3 phase wasn't detected in the entire XRD images. This is because B_2O_3 as sintering aid is amorphous state thus it has no diffraction peaks in the XRD. Furthermore, the melting point of B_2O_3 is 445 °C, which forms a liquid phase during the sintering process, and the liquid phase in higher temperatures was coated around the grains. In our previous works [18–20], the XRD results are also have no B_2O_3 diffraction peaks.

In order to clarify the effects of sintering temperatures and the amount of B_2O_3 doping on the microstructures of $ZnTiNb_2O_8$ compounds, the morphological changes of the 1 wt% B_2O_3-doped $ZnTiNb_2O_8$ compounds sintered at different temperatures and samples with various B_2O_3 addition sintered at 1050 °C were investigated as representatives. The surface micrographs of $ZnTiNb_2O_8$ samples with 1 wt% B_2O_3 at different sintering temperatures were shown in Fig. 4(a)–(d). For 1000 °C, the particles of ZTN samples were small, some pores could be easily observed (Fig. 4(a)). At 1050 °C, the homogeneously fine microstructures with quite uniform size (about 2 μm) and almost no pores were observed in Fig. 4(b). However, with the temperature increasing further, abnormal rapid grain growth appeared (Fig. 4(c)), some grain boundary melted (Fig. 4(d)), thus the dense microstructure with low porosity disappeared, which were consistent with the curves of the apparent densities and diametric shrinkage in Fig. 1. From the above analyses, it was obvious that $ZnTiNb_2O_8$ ceramics were successfully prepared with high density at 1050 °C.

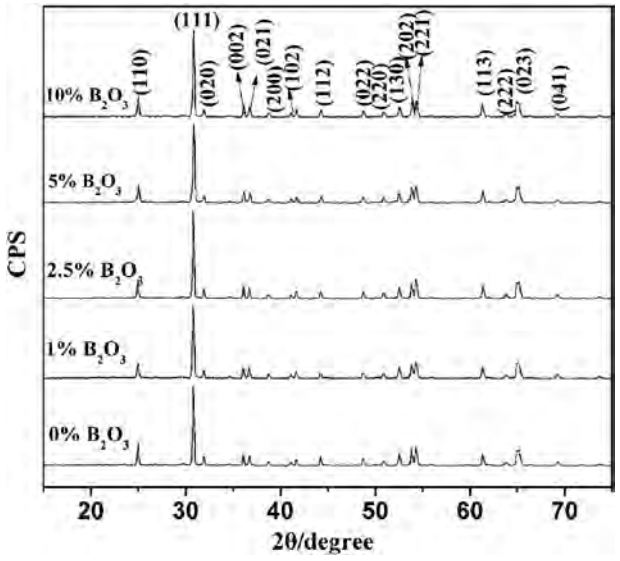

Fig. 3. The X-ray diffraction patterns of the $ZnTiNb_2O_8$ samples with different amounts of B_2O_3 additive sintered at 1050 °C.

The surface micrographs of the samples with different amounts of B_2O_3 doping sintered at 1050 °C were shown in Fig. 5(a)-(d). As can be seen in Fig. 5, the grain grew quickly and a number of pores appeared with the increase of B_2O_3 addition. At the level of 1–2.5 wt%B_2O_3 addition, nearly full dense specimens were obtained with the grain size ~2 μm as shown in Fig. 5(a), (b). In addition, with the amount of B_2O_3 up to 5 wt% abnormal grain growth can be found as shown in Fig. 5(c), and when the doping of B_2O_3 increase to 10 wt%, obvious grain boundary melting appeared shown in Fig. 5(d). Thus, small amount of B_2O_3 doping played an important role in reducing the sintering temperature due to the significant effect of liquid-phase sintering mechanism. However, with the amount of B_2O_3 addition increasing further, such as 5 wt %-B_2O_3-doped, some pores appeared again due to the evaporation of liquid phase.

The changes of ε_r and $Q\cdot f$ as a function of sintering temperatures at different B_2O_3 contents from 1 to 10 wt% are shown in Fig. 6. As shown in Fig. 6(a), the relationships between dielectric constant and sintering temperature of ZTN samples appeared the same trend and were irrelevant to the variation of B_2O_3 doping, which was consistent with the tendency of apparent density due to a fact that a higher density was corresponding to a lower porosity. The increase in ε_r values was attributed to a higher density as well as a lower porosity. The highest ε_r values of 35.04 was obtained for 1 wt % B_2O_3-added specimen sintered at 1050 °C which was significantly comparable with the results reported by the solid-state method [6–9]. Moreover, ε_r values was decreased slightly with the increase of B_2O_3 content due to a reduction in the density. In addition, the decrease of ε_r values at high B_2O_3 doping level might be also result from a low ε_r value of sintering aid B_2O_3 ($\varepsilon_r = 3$–8).

To clarify effects of crystal structure on dielectric constant, theoretical dielectric polarizability ($\alpha_{theo.}$) was calculated to be 28.99 according to additive rule with ionic polarizability of composing ions or oxides [23] as formulated in Eq. (2). While observed dielectric polarizability ($\alpha_{obs.}$) was calculated to be 29.12 by Clausius-Mossotti equation as formulated in Eq. (3) with measuring dielectric constant at microwave frequencies [24], which was same with the previous study [6]. This also demonstrated that B_2O_3 doping has no negative effect on dielectric constant. By comparison values of $\alpha_{theo.}$ and $\alpha_{obs.}$ were in good agreement with each other, and the minor deviation between the $\alpha_{obs.}$ and $\alpha_{theo.}$ could be attributed to relative density because the $\alpha_{obs.}$ value depended on specimens and fabrication process.

$$\alpha_{theo} = \alpha(ZnTiNb_2O_8) = \alpha(ZnO) + \alpha(TiO_2) + \alpha(Nb_2O_5) \quad (2)$$

$$\alpha_{obs} = \frac{1}{b} V_m \frac{\varepsilon - 1}{\varepsilon + 2} \quad (3)$$

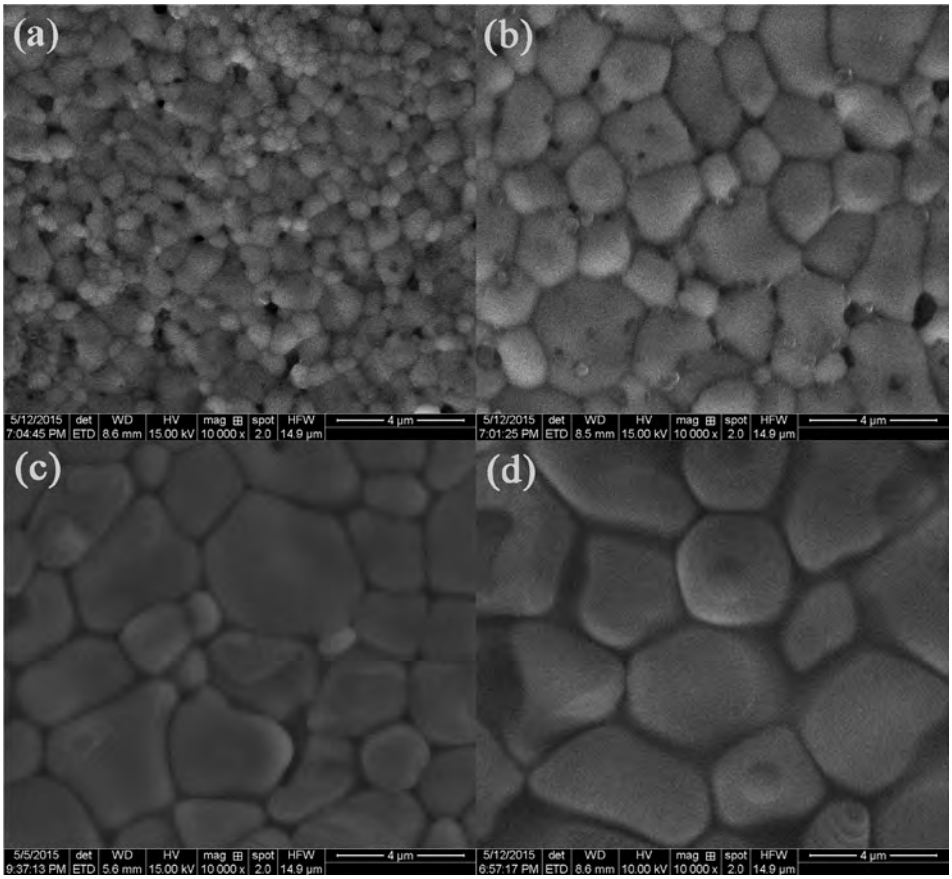

Fig. 4. The SEM micrographs of $ZnTiNb_2O_8$ samples with 1 wt% B_2O_3 sintered at different temperatures (a-d corresponding to 1000 °C 1050 °C 1100 °C 1150 °C).

Where α *(ZnO)*, α *(Nb_2O_5)*, and α *(TiO_2)* represented oxides polarizabilities reported by Shannon [24]. Moreover, V_m, ε and b indicated the molar volume of samples, dielectric constant and constant value ($4\pi/3$), respectively.

The quality factors of ZTN ceramics were measured by the reflection cavity method. The $Q\cdot f$ values of ZTN ceramics with different amounts of B_2O_3 additions as a function of sintering temperatures are illustrated in Fig. 6(b). The 1 wt%-B_2O_3-doped and 2.5 wt%-B_2O_3-doped specimens showed the similar tendency with those of dielectric constant. The $Q\cdot f$ values increased from 25,600 to 50,100 GHz then decreased slightly in the sintering temperature region of 1000–1150 °C. The remarkable increase in $Q\cdot f$ values ranging from 1000 to 1050 °C was also related to the reduction of porosity according to results of SEM microstructures shown in Fig. 4(a-b). It was well known that porosity, secondary phase and structure defect of ceramics as extrinsic factors usually produced a deterioration in $Q\cdot f$ values [25,26]. Among these factors, the porosity was suggested to affect $Q\cdot f$ values obviously below 1050 °C. The decline of $Q\cdot f$ value mainly caused by the non-uniform micro-structure by abnormal grain growth. Moreover, the accumulation of the impurities and the secondary phase also made $Q\cdot f$ value decreasing. The saturated $Q\cdot f$ value was ~50,100 GHz obtained at 1050 °C, which was significantly higher than the results reported by the solid-state method [15,21,22]. For example, Kim et al. [15] reported a $Q\cdot f$ value of 33,000 GHz by the solid-state technique.

When doping ratio increased to 5 wt%, $Q\cdot f$ values increased firstly and then decreased roughly with the increase of the sintering temperature. A maximum $Q\cdot f$ value can also be obtained at 1050 °C. However, the $Q\cdot f$ value was too poor to be detected at 1100 °C. The dielectric loss of ZTN ceramics with 5 wt% B_2O_3 addition sintered at 1100 °C was very high and the resonance peak couldn't be detected. It may be caused by the different sintering process, microcracks, and the accidental error. Meanwhile the dielectric constant of this point also have a slight decline. Therefore statistical analysis should be applied in our study to avoid the similar situation in the future. The curve of 10 wt%-B_2O_3-doped ZTN ceramics showed same tendency with that of 1 wt% and 2.5 wt%-B_2O_3-doped ZTN ceramics whereas the $Q\cdot f$ value of 10 wt% B_2O_3 sintered at 1150 °C also had a poor value. This may be caused by excess of B_2O_3 doping and extreme high sintering temperatures [27,28]. In general, several factors contribute to the dielectric loss at microwave frequencies and these factors can be divided into two parts: the intrinsic loss and the extrinsic loss. Intrinsic losses are mainly caused by lattice vibration modes while extrinsic losses are dominated by second phases, oxygen vacancies, grain sizes and densification or porosity. Thus the more B_2O_3 was doped, the lower $Q\cdot f$ value was.

Generally, the electronic components should possess a near-zero temperature coefficient of resonant frequency. The temperature coefficient of resonant frequency (τ_f) is related to temperature coefficient of dielectric constant (τ_ε) and the linear thermal expansion coefficient (α_L) as Eq. (4).

$$\tau_f = -\alpha_L - \frac{1}{2}\tau_\varepsilon \tag{4}$$

where the linear thermal expansion coefficient (α_L) is in the range of 10 ppm/°C for all the ceramics [25]. So τ_f mainly depends on temperature coefficient of dielectric constant (τ_ε). From the macroscopic Clausius-Mosotti equation, the temperature

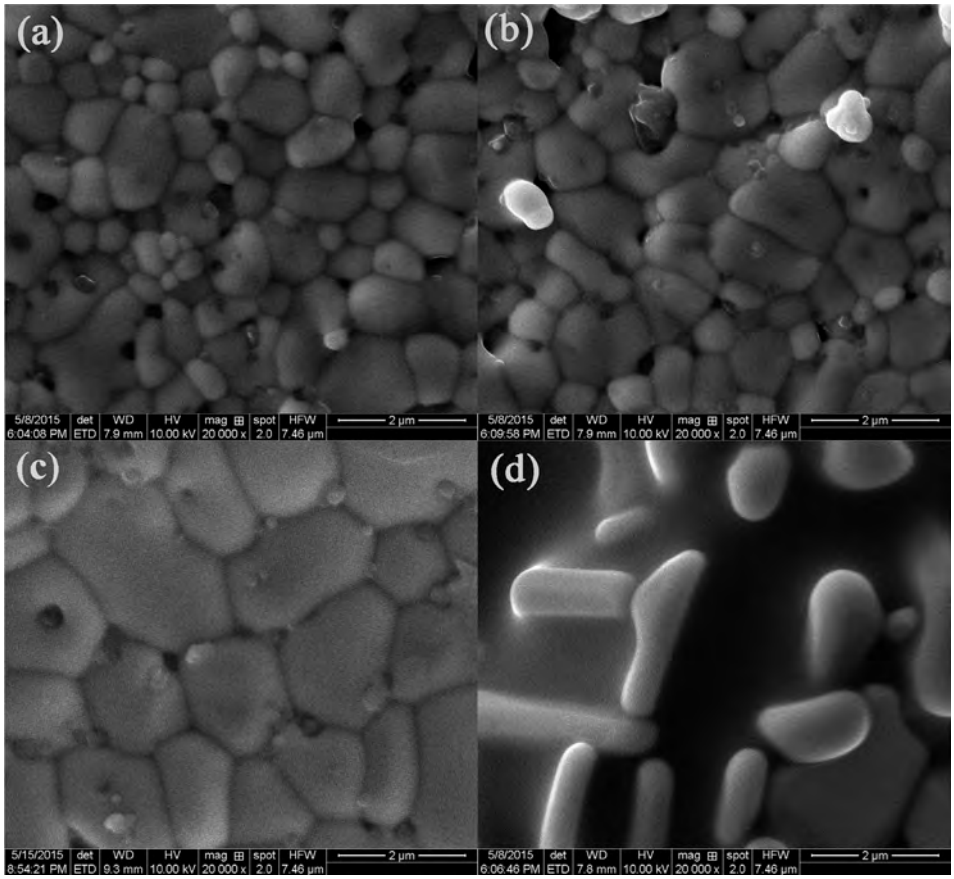

Fig. 5. The SEM micrographs of $ZnTiNb_2O_8$ samples with different amounts of B_2O_3 doping sintered at 1050 °C (a-d corresponding to 1 wt% 2.5 wt% 5 wt% 10 wt%).

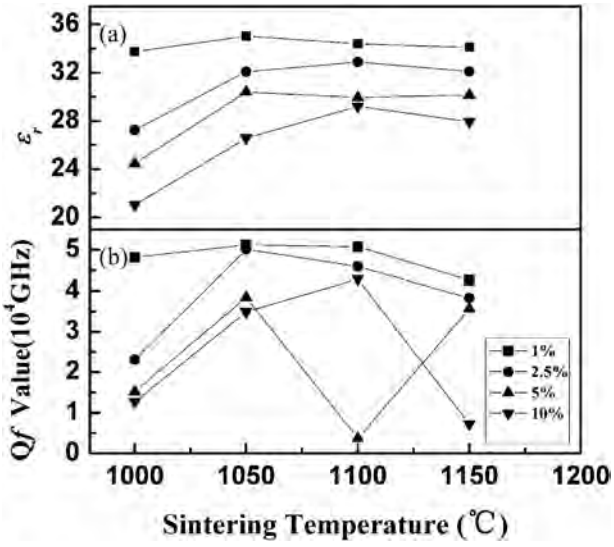

Fig. 6. The changes of ε_r and $Q{\cdot}f$ as a function of sintering temperatures at different B_2O_3 contents from 1 to 10 wt%.

coefficient of dielectric constant can be derived as Eq. (5).

$$\tau_\varepsilon = \frac{1}{\varepsilon_r}\left(\frac{\partial \varepsilon_r}{\partial T}\right) = \frac{(\varepsilon_r - 1)(\varepsilon_r + 2)}{3\varepsilon_r} \times \left[\frac{1}{\alpha_m}\left(\frac{\partial \alpha_m}{\partial T}\right)_V + \frac{1}{\alpha_m}\left(\frac{\partial \alpha_m}{\partial V}\right)_T \left(\frac{\partial V}{\partial T}\right)_P - \frac{1}{V}\left(\frac{\partial V}{\partial T}\right)_P\right] \quad (5)$$

where α_m and V indicated the polarizability and volume of a small sphere, respectively. According to Bosman and Havinga [29], the second and third terms in the square brackets are related to the volume expansion, which have nearly equal magnitude and opposite sign. Therefore, the effect of these terms is negligible and the τ_ε is mainly dependent on the first part.

Moreover, the τ_f values of ZTN ceramics as a function of B_2O_3 content were illustrated in Fig. 7. As can be seen, all the τ_f values were fluctuated around −20 ppm/°C, ranging from −10.21 to −32.2 ppm/°C, which were lower than the τ_f of pure ZTN -52 ppm/°C [6]. Although the mechanism of the τ_f values was unclear now, it could be reasonably believed that the liquid phase should be responsible for the variation of the τ_f values and the addition of appropriate B_2O_3 could adjust the τ_f values of ZTN ceramics to zero. However, when the doping of B_2O_3 increase to 10 wt %, unknown secondary appeared and obvious grain boundary melting appeared due to excessive liquid phase. Thus, the τ_f values lower than 5 wt% B_2O_3 doped. In our previous works about B_2O_3 additives [18,19], similar result were observed. Hence, it was obvious that the improvement in the τ_f value was required for the dielectric resonator applications at high frequency.

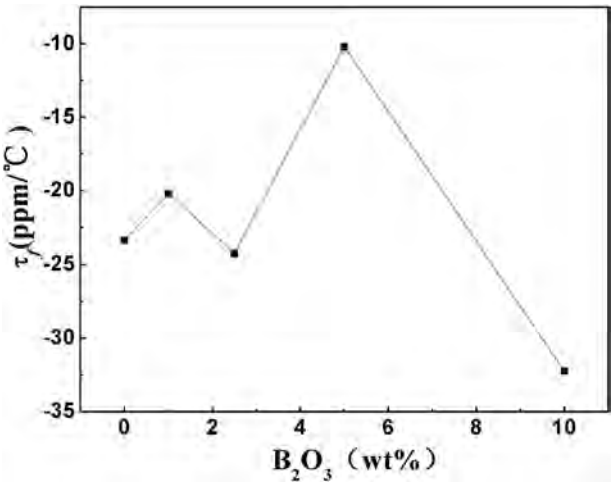

Fig. 7. The τ_f values of $ZnTiNb_2O_8$ ceramics as a function of B_2O_3 content.

4. Conclusion

The effect of B_2O_3 doping on the microwave dielectric properties and microstructure of $ZnTiNb_2O_8$ compounds at various sintering temperatures was investigated in this study. The XRD patterns of $ZnTiNb_2O_8$ compounds showed the ordered ixiolite-structure corresponding to the JADE card (JCPDS# 48-0323), for space group *Pbcn* (60), unit cell molecular number Z = 1. The excess of B_2O_3 doping and higher sintered temperatures had detrimental effect on the microwave properties. It was found that 1 wt% B_2O_3 doping was effective in reducing the sintering temperature of $ZnTiNb_2O_8$ compounds without any detrimental effect on microwave dielectric properties. The excellent microwave properties, the $Q{\cdot}f$ value of ~50,100 GHz, the ε_r value of ~35.04, and the τ_f value of ~ -20.21 ppm/°C, were obtained for $ZnTiNb_2O_8$ compound with 1 wt% B_2O_3 sintered at 1050 °C.

Acknowledgments

This work was supported by the Project Development Plan of Science and Technology of Ji'nan City (No.201303061), Ji'nan City Youth Science and Technology Star Project (No.2013035), National Natural Science Foundation (No.51472108) and Study Abroad Programs by Shandong Province Government.

References

[1] Terrell A. Vanderah, Science 298 (2002) 1182–1184.
[2] C.L. Huang, J.Y. Chen, J. Am. Ceram. Soc. 92 (2009) 379–383.
[3] H.T. Wu, L.P. Zhao, J. Univ. Jinan (Sci. Tech.) 30 (2016) 177–183.
[4] T. Takada, S.F. Wang, S. Yoshikawa, et al., J. Am.Ceram. Soc. 77 (1994) 1909.
[5] Q.W. Liao, L.X. Li, Dalton. Trans. 41 (2012) 6963–6969.
[6] Q.J. Mei, C.Y. Li, J.D. Guo, H.T. Wu, J. Alloys. Compd. 626 (2015) 217–222.
[7] E.Z. Li, P. Zhang, S.X. Duan, et al., J. Alloys. Compd. 647 (2015) 866–872.
[8] W. Wang, L.Y. Li, S.M. Xiu, et al., J. Alloys. Compd. 639 (2015) 359–364.
[9] Q. Xu, D. Zhan, D. Ping, et al., J. Alloys. Compd. 558 (2013) 77–83.
[10] C.H. Shen, C.L. Huang, L.M. Lin, et al., J. Alloys. Compd. 504 (2010) 228–232.
[11] B.W. Hakki, P.D. Coleman, IEEE Trans. 8 (1960) 402–410.
[12] W.E. Courtney, IEEE Trans. 18 (1970) 476–485.
[13] D.W. Kim, J.H. Kim, J.R. Kim, et al., Jpn. J. Appl. Phys. 40 (2001) 5994.
[14] Z.L. Huan, Q.C. Sun, W.B. Ma, et al., J. Alloys. Compd. 551 (2013) 630–635.
[15] D.W. Kim, H.B. Hong, K.S. Hong, Jpn. Soc. Appl. Phys. 41 (2002) 1465–1469.
[16] Y. Lei, Y.S. Yin, Y.C. Liu, Adv. Mater. Res. 217–208 (2011) 1235–1238.
[17] Q.W. Liao, L.X. Li, Dalton Trans. 41 (2012) 6963–6969.
[18] H.T. Wu, Q.J. Mei, J. Alloy. Compd. 651 (2015) 393–398.
[19] H.T. Wu, J.D. Guo, J.X. Bi, Q.J. Mei, J. Alloy. Compd. 661 (2016) 535–540.
[20] H.T. Wu, L.X. Li, J. Sol-Gel Sci. Technol. 58 (2011) 48–55.
[21] C.F. Tseng, P.H. Chen, P.A. Lin, J. Alloys. Compd. 632 (2015) 810–815.
[22] D.X. Zhou, G. Dou, M. Guo, J. Alloys. Compd. 130 (2011) 903–908.
[23] R.D. Shannon, G.R. Rossman, Am. Min. 77 (1992) 94–100.
[24] R.D. Shannon, J. Appl. Phys. 73 (1993) 348–366.
[25] L.X. Li, H. Sun, H.C. Cai, X.S. Lv, J. Alloys Comp. 639 (2015) 516–519.
[26] Z.K. Song, P. Zhang, Y. Wang, L.X. Li, J. Alloys Comp. 583 (2014) 546–549.
[27] B.J. Li, J.Y. Chen, G.S. Huang, J. Alloy. Compd. 505 (2010) 291–296.
[28] Y. Lv, R.Z. Zuo, Ceram. Int. 39 (2013) 2545–2550.
[29] A.J. Bosman, E.E. Havinga, Phys. Rev. 129 (1963) 1593–2000.